THE JOURNAL OF BIOLOGICAL CHEMISTRY VOL. 289, NO. 44, pp. 30237–30248, October 31, 2014
Published in the U.S.A.

The Arf6 GTPase-activating Proteins ARAP2 and ACAP1 Define Distinct Endosomal Compartments That Regulate Integrin $\alpha5\beta1$ Traffic*

Received for publication, July 11, 2014, and in revised form, September 9, 2014 Published, JBC Papers in Press, September 15, 2014, DOI 10.1074/jbc.M114.596155

Pei-Wen Chen, Ruibai Luo, Xiaoying Jian, and Paul A. Randazzo[1]

From the Laboratory of Cellular and Molecular Biology, NCI, National Institutes of Health, Bethesda, Maryland 20892

Background: Arf6 has a number of distinct effects on trafficking of integrins.
Results: Two Arf6 GAPs, ARAP2 and ACAP1, were distinctly localized and had differential effects on integrin trafficking and integrin adhesions.
Conclusion: Arf6 effects on integrins are determined by associated Arf6 GAPs.
Significance: Arf GAPs define control points of integrin traffic important to cellular behaviors related to invasion and metastasis in cancer.

Arf6 and the Arf6 GTPase-activating protein (GAP) ACAP1 are established regulators of integrin traffic important to cell adhesion and migration. However, the function of Arf6 with ACAP1 cannot explain the range of Arf6 effects on integrin-based structures. We propose that Arf6 has different functions determined, in part, by the associated Arf GAP. We tested this idea by comparing the Arf6 GAPs ARAP2 and ACAP1. We found that ARAP2 and ACAP1 had opposing effects on apparent integrin $\beta1$ internalization. ARAP2 knockdown slowed, whereas ACAP1 knockdown accelerated, integrin $\beta1$ internalization. Integrin $\beta1$ association with adaptor protein containing a pleckstrin homology (PH) domain, phosphotyrosine-binding (PTB) domain, and leucine zipper motif (APPL)-positive endosomes and EEA1-positive endosomes was affected by ARAP2 knockdown and depended on ARAP2 GAP activity. ARAP2 formed a complex with APPL1 and colocalized with Arf6 and APPL in a compartment distinct from the Arf6/ACAP1 tubular recycling endosome. In addition, although ACAP1 and ARAP2 each colocalized with Arf6, they did not colocalize with each other and had opposing effects on focal adhesions (FAs). ARAP2 overexpression promoted large FAs, but ACAP1 overexpression reduced FAs. Taken together, the data support a model in which Arf6 has at least two sites of opposing action defined by distinct Arf6 GAPs.

Endocytic traffic of transmembrane proteins, including cell adhesion molecules such as integrins, is emerging as a critical pathway in cell migration and signaling related to cancer invasion and metastasis (1). Arf6, a GTPase of the Ras superfamily, is a central component of the regulatory machinery controlling the relevant endocytic trafficking (2–4). However, the trafficking pathways and the site of Arf6 action are now appreciated to be more complex than prevailing paradigms. The understanding of processes such as invasion and metastasis will be advanced by further description of the relationship between Arf6 and the range of itineraries possible for cargos such as integrins.

Distinct endocytic compartments and the connections between them are continuing to be discovered. In the prevailing paradigms, endocytosed cargos are translocated to a common sorting compartment from which they are directed toward the degradative pathway or either a fast or slow recycling pathway (5, 6). This description is now understood to be an oversimplification, with recent descriptions of integrins being recycled from the degradative pathway (7) and other cargos bypassing the common sorting early endosome for direct transfer to the Arf6/Rab22 tubular recycling endosome (8). Therefore, the pre-early endosome may be a critical sorting station for determining the endocytic itinerary. One class of pre-early endosomes defined by the presence of adaptor protein containing PH[2] domain, phosphotyrosine-binding (PTB) domain, and leucine zipper motifs 1 and 2 (APPL1/2) has been found to traffic integrins (9).

An understanding of the mechanism of Arf6 function within the endocytic recycling compartment has remained elusive, as has been the effect of Arf6-dependent recycling of the cargo integrin on cellular structures and behaviors. Arf6 has been reported to accelerate the recycling of cargo, including transferrin and integrin $\alpha5\beta1$ (10–12). However, it slows the recycling of integrin $\alpha v\beta3$ (12), the opposite of the effect on integrin $\alpha5\beta1$. In addition, Arf6 has been reported to increase the endocytosis of integrin $\alpha5\beta1$ (13). Adding to the complexity are the reported cellular effects of Arf6-dependent endocytic traffic. Focal adhesions (FAs) are structures that mediate the attachment of cells to the extracellular matrix. FAs contain clustered integrins that bind the extracellular matrix and a cytoplasmic plaque that connects the integrins to the actin cytoskeleton and is comprised of hundreds of structural and signaling proteins, including vinculin and paxillin (14). Arf6-induced endocytosis

* This work was supported by the intramural program of the NCI, National Institutes of Health (Project BC 007365).

[1] To whom correspondence should be addressed: Laboratory of Cellular and Molecular Biology, National Cancer Institute, Bldg. 37, Rm. 2012, Bethesda, MD. Tel.: 301-496-3788. E-mail: randazzp@mail.nih.gov.

[2] The abbreviations used are: PH, pleckstrin homology; FA, focal adhesion; GAP, GTPase-activating protein; Ab, antibody; EGFP, enhanced GFP; FRAP, fluorescence recovery after photobleaching.

of integrin $\alpha5\beta1$ has been reported to result in a loss of FAs (13), which would be anticipated given less integrin on the cell surface to cluster. However, it has also been reported that Arf6-driven recycling of integrin $\alpha5\beta1$ destabilizes FAs (12) despite having a greater concentration of integrins on the cell surface. Reconciling these apparently contradictory results will require a more detailed understanding of the site or sites of Arf6 action and the specific endocytic itineraries that may be affected by each.

Examination of Arf GAPs may provide insights into the complexities of Arf6-regulated endocytic traffic of integrins. Arf GAPs, with 31 genes and multiple splice variants, outnumber the five Arfs in humans (15, 16). Of the Arf GAPs, several specific for Arf6 have been described, including ACAP1, ACAP2, and ARAP2 (17, 18). ArfGAPs are multidomain proteins that have been speculated to have effector functions (19–21). Either by responding to specific signals, by associating with distinct Arf6 compartments, or through an effector function, the Arf6 GAPs could determine specific functions of Arf6.

We test the idea that Arf6 GAPs, at least in part, determine the specific effect of Arf6 on endocytic traffic by comparing ARAP2 and ACAP1 (see Fig. 1*A* for a schematic of domain structures). The proteins are structurally distinct. ARAP2 is comprised of a sterile α-motif domain, five PH domains, an Arf GAP domain, an Ank repeat domain, an inactive Rho GAP domain, and a Ras association domain. ACAP1 is comprised of a *Bin/Amphiphysin/Rvs* domain, a PH domain, an Arf GAP domain, and an Ank repeat domain. ACAP1 has already been found to accelerate the recycling of integrins and to be associated with the tubular recycling compartment containing Rab11 (17, 22). We find important differences between ARAP2 and ACAP1 in the effects on integrin traffic, effects on FAs, and the associated endocytic compartments. The results support a model in which Arf function is determined, in part, by the associated Arf GAP and leads to the identification of a unique APPL/Arf6/ARAP2 compartment.

MATERIALS AND METHODS

Plasmids, Antibodies, and Reagents—Mammalian expression vectors for N-terminal FLAG-tagged ARAP2, [R728K]ARAP2, and ACAP1 have been described previously (17, 18). Rab21-mCherry and GFP-ACAP1 were gifts from Dr. Elizabeth Sztul (University of Alabama at Birmingham, Birmingham, AL) and Dr. Victor Hsu (Harvard Medical School, Boston, MA), respectively. GFP-human APPL1 was purchased from Addgene (Addgene plasmid 22198). Rabbit anti-ARAP2 antiserum (antiserum 1186) were raised against the same synthetic peptide, RSRTLPKELQDEQILK, as antisera 1185 described previously (18) (Covance Research, Princeton, NJ). 1186 antisera were affinity-purified with a purification kit (Thermo Scientific, Lafayette, CO) using the peptide against which the antibody was raised. Affinity-purified 1186 antisera detected a band at 190 kDa by Western blotting. The band at 190 kDa was diminished in three cell lines treated with siRNA targeting ARAP2, providing evidence that this 190-kDa species was endogenous ARAP2. Anti-FLAG polyclonal Ab, anti-Vinculin monoclonal Ab (catalog no. hVIN-1), primaquine, and fibronectin were purchased from Sigma-Aldrich (St. Louis, MO). Anti-$\beta1$ integrin monoclonal Ab (clone MEM101A-PE) was from Novus Biologicals (Littleton, CO). Anti-active $\beta1$ integrin monoclonal Ab (clone 9EG7), anti-inactive $\beta1$ integrin monoclonal Ab (clone MAB13), anti-EEA1 monoclonal Ab, and anti-actin monoclonal Ab were from BD Biosciences. Anti-active $\beta1$ integrin monoclonal Ab (clone 12G10-FITC), anti-GFP monoclonal Ab, and anti-APPL polyclonal Ab were from Abcam (Cambridge, MA). Anti-FLAG monoclonal Ab and anti-EGFR rabbit polyclonal Ab were from Cell Signaling Technology (Danvers, MA). Anti-GFP and Hsc70 monoclonal Abs were from Covance Research and Santa Cruz Biotechnology (Dallas, TX), respectively. Alexa Fluor-labeled secondary antibodies were from Invitrogen. Horseradish-peroxidase-conjugated anti-mouse and anti-rabbit IgG Abs were from Bio-Rad.

Cell Culture and Transfection—HeLa and MDA-MB-231 cells were maintained at 37 °C in Dulbecco's modified Eagle's medium and RPMI 1640 medium supplemented with 100 units/ml penicillin, 100 μg/ml streptomycin, and 10% FBS. siRNA against ARAP2 (5′-GUAAGAAGACAUUGGGUUA-3′), ACAP1 siGENOME SMARTpool, and control siRNA (siCONTROL non-targeting siRNAs #2 and #4) were purchased from Thermo Scientific (Lafayette, CO). Subconfluent cells were transfected with 40 nM siRNA using DharmaFECT transfection reagent 1 (Thermo Scientific). Functional experiments with siRNA-transfected cells were performed 72 h following transfection when ARAP2 and ACAP1 expression was reduced. FLAG-ACAP1 expression was reduced 77% in ACAP1 siRNA-transfected cells compared with control siRNA-transfected cells. For experiments requiring exogenous protein expression, 48 h after siRNA transfection, cells were transfected with plasmids expressing FLAG-ARAP2, FLAG-[R728K]-ARAP2, $\alpha5$ integrin-EGFP, untagged $\beta1$ integrin, Rab5-GFP, Rab21-mCherry, Rab4-HA, Rab11-GFP, or GFP using Lipofectamine 2000 reagent (Invitrogen) or the Amaxa nucleofector system (Amaxa Inc., Gaithersburg, MD) according to the instructions of the manufacturer. 24 h later, the effects on integrins and FAs were assessed using confocal microscopy.

Integrin Internalization Assay—Integrin internalization and recycling were followed in complex with antibodies to integrin $\beta1$ and detected with secondary antibody for FACS (23) and immunofluorescence experiments. To study internalization, cells were incubated at 4 °C with R-phycoerythrin (PE)- or FITC-conjugated anti-$\beta1$ integrin (clones MEM101A and 12G10, respectively) antibody at 5 μg/ml for 30 min. Cells were washed to remove unbound antibody. Internalization was initiated by adding medium (37 °C). At each time point, cells were put on ice, washed with ice-cold PBS + 0.2% BSA, and incubated at 4 °C for 30 min with Alexa Fluor 647 anti-mouse antibody in cold PBS + 0.2% BSA to detect the remaining cell surface primary antibody. Cells were washed, detached from plates using StemPro Accutase (Invitrogen), and analyzed using flow cytometry (BD FACSCalibur, BD Biosciences). The ratio of normalized fluorescence intensity from integrin antibody on the cell surface at each time point (signal from secondary Ab) and total surface integrin labeled by antibody at time 0 (signal from primary integrin Ab) was determined. For the internalization assay using MAB13 Ab (inactive $\beta1$ integrin) that was

unconjugated to a fluorophore, all procedures were the same, except the signal was normalized to time 0.

Transferrin Recycling Assay—Cells were incubated for 30 min with 0.025 μg/ml Transferrin-Alexa Fluor 488 (Invitrogen) in media. Cells were washed three times with ice-cold PBS and incubated in media at 37 °C for the indicated times. Cells were transferred on ice, washed, and detached for FACS as described for integrin. The recycled transferrin was calculated as 100% minus the percentage of cell-associated signal at time 0.

EGFR Degradation—siRNA-treated HeLa cells were serum starved overnight in DMEM+0.1% FBS and treated with 100 ng/ml EGF for the times indicated. Cells were lysed in lysis buffer (50 mM Tris-HCl (pH 7.5), 150 mM NaCl, 1 mM EDTA, and 1% Triton X-100 supplemented with protease and phosphatase inhibitor mixture), and 20 μg of lysates were subjected to Western blotting using anti-EGFR antibody.

Immunoprecipitation and Western Blotting—Cells were lysed in lysis buffer. Proteins were immunoprecipitated using either anti-FLAG antibody conjugated to agarose or anti-GFP and anti-ARAP2 antibody precipitated with protein A/G-agarose. Immunoblots were processed by standard methods and visualized with enhanced chemiluminescence.

Immunofluorescence and Confocal Microscopy—Cells were plated on coverslips coated with 10 μg/ml fibronectin and fixed in 4% paraformaldehyde. For AlF_4^- treatment, cells were incubated in media containing 30 mM NaF and 50 μM $AlCl_3$ for 30 min before fixation. Fixed cells were incubated in 15 mM glycine for 10 min and 50 mM NH_4Cl for 2 × 10 min and then permeabilized and blocked with 0.2% saponin, 0.5% BSA, and 1% FBS in PBS for 20 min. Cells were incubated in primary antibody for 1 h, followed by secondary antibodies for 1 h, and mounted in DakoCytomation fluorescent mounting medium (Dako, Carpinteria, CA). Images for fixed cells were taken on a Zeiss LSM 510 attached to a Zeiss Axiovert 100 M with a 63 × 1.4 numerical aperture plan Neofluar oil immersion lens (Carl Zeiss, Thornwood, NY). For FRAP, the cells were plated on a Lab-TekII four-chambered coverglass coated with fibronectin and visualized with a Zeiss Axiovert 200 microscope and PerkinElmer Life Sciences UltraView spinning disk confocal system using a 63 × 1.4 numerical aperture plan Neofluar oil immersion objective. Cells were imaged in real time on a stage preheated to 37 °C with a CO_2 chamber using an Orca-ERII camera (Hamamatsu, Bridgewater, NJ). α5-Integrin-EGFP-labeled adhesions were bleached using a 488-nm laser at full power. During fluorescence recovery, images were captured at 200- to 500-ms intervals for less than 5 min at a reduced laser intensity (40∼60%) to minimize undesired photobleaching. FRAP data were fit to exponential curves using GraphPad Prism (La Jolla, CA).

Image Analysis and Statistics—Focal adhesion number per cell was analyzed using ImageJ (National Institutes of Health, http://rsb.info.nih.gov/ij/) as described previously (24). For analysis of photobleaching recovery, the integrated fluorescence intensity was recorded in prebleach and recovery image series and normalized so that the prebleach value was 100%. The recovery halftime ($t_{1/2}$) and mobile fraction were calculated using the normalized recovery values with the one-phase exponential association fit in GraphPad Prism (GraphPad Software). For quantification of the colocalization of integrins with endosomal markers, z stack images of consecutive optical planes spaced by 0.5 μm were acquired to cover the whole cell volume using confocal microscopy. Pearson's coefficient was determined using Imaris 7.4.0. The differences between multiple and two treatments were analyzed by one-way analysis of variance using Bonferroni's multiple comparison test and Student's *t* test, respectively, with $p < 0.05$ considered to be significant.

RESULTS

ARAP2 Affects Endocytosis and Recycling of Integrins Differently Than ACAP1—Arf6·GTP can have opposing effects on integrin traffic and integrin-dependent cell behaviors. Arf6·GTP has been reported to accelerate integrin recycling with an increase in integrin-based cell adhesion (11, 25, 26), and it has also been reported to decrease cell adhesion because of increased integrin internalization, leading to a loss of FAs (13, 27). These apparently contradictory results may be explained by binding of Arf6·GTP to different effectors and/or functioning of Arf6·GTP at multiple sites. One Arf6 GAP, ACAP1, not associated with FAs, promotes recycling of integrins. Three other *bona fide* Arf6 GAPs, ARAP2 and GIT1/2, reside in and regulate FAs, but their effects on integrin traffic have not been examined. Here we examined ARAP2 and ACAP1. We hypothesize that differential effects of Arf6 are mediated, at least in part, by interacting with structurally distinct Arf6 GAPs. In an initial test of this idea, we compared the effect of ACAP1 and ARAP2 knockdown on the net internalization rate of integrin β1, examined for 30 min. Integrins are found in at least two states: an active form, which has a high affinity for extracellular matrix ligands, and an inactive form that has a low affinity for extracellular matrix ligands. The two forms have different conformations and can be distinguished by binding to specific antibodies. We first focused on the active form of integrin β1. An antibody specific for active β1 was used to measure the endocytosis of integrin (23). Knockdown of ACAP1 reduced the surface levels of active integrin β1 by 13.7 ± 0.02%. Total cell-associated active β1 integrin was also decreased by 17.1 ± 0.06% (Fig. 1*B*). The ratio of surface to total integrin was not changed. Cells with reduced ACAP1 internalized a greater fraction of integrin β1 after 20 min of internalization. After 30 min, there was 34% greater internalization of integrin β1 compared with controls. This result is consistent with reduced recycling through the Rab11 (slow) recycling pathway that has been reported for ACAP1 knockdown (Fig. 1*C*) (22, 28). ARAP2 knockdown was different from ACAP1 knockdown in two respects. First, ARAP2 knockdown cells had a greater content of integrin β1, whereas ACAP1 knockdown cells had a small decrease in integrin β1 content. Surface levels of active β1 integrin were increased ∼2-fold in ARAP2 siRNA-treated HeLa (Fig. 1*E*) and MDA-MB-231 cells (Fig. 2*A*). Total cell-associated active β1 integrin was also increased ∼2-fold in ARAP2 knockdown cells (Figs. 1*E* and 2*A*). Consequently, the ratio of surface to total integrin was not affected (48 ± 3.1% for control *versus* 44 ± 7.1% for ARAP2 knockdown in HeLa cells and 14 ± 1.7% *versus* 14 ± 0.4% in MDA-MB-231 cells). The second difference between ARAP2 and ACAP1 knockdown was in the internalization of integrins. In ARAP2 knockdown

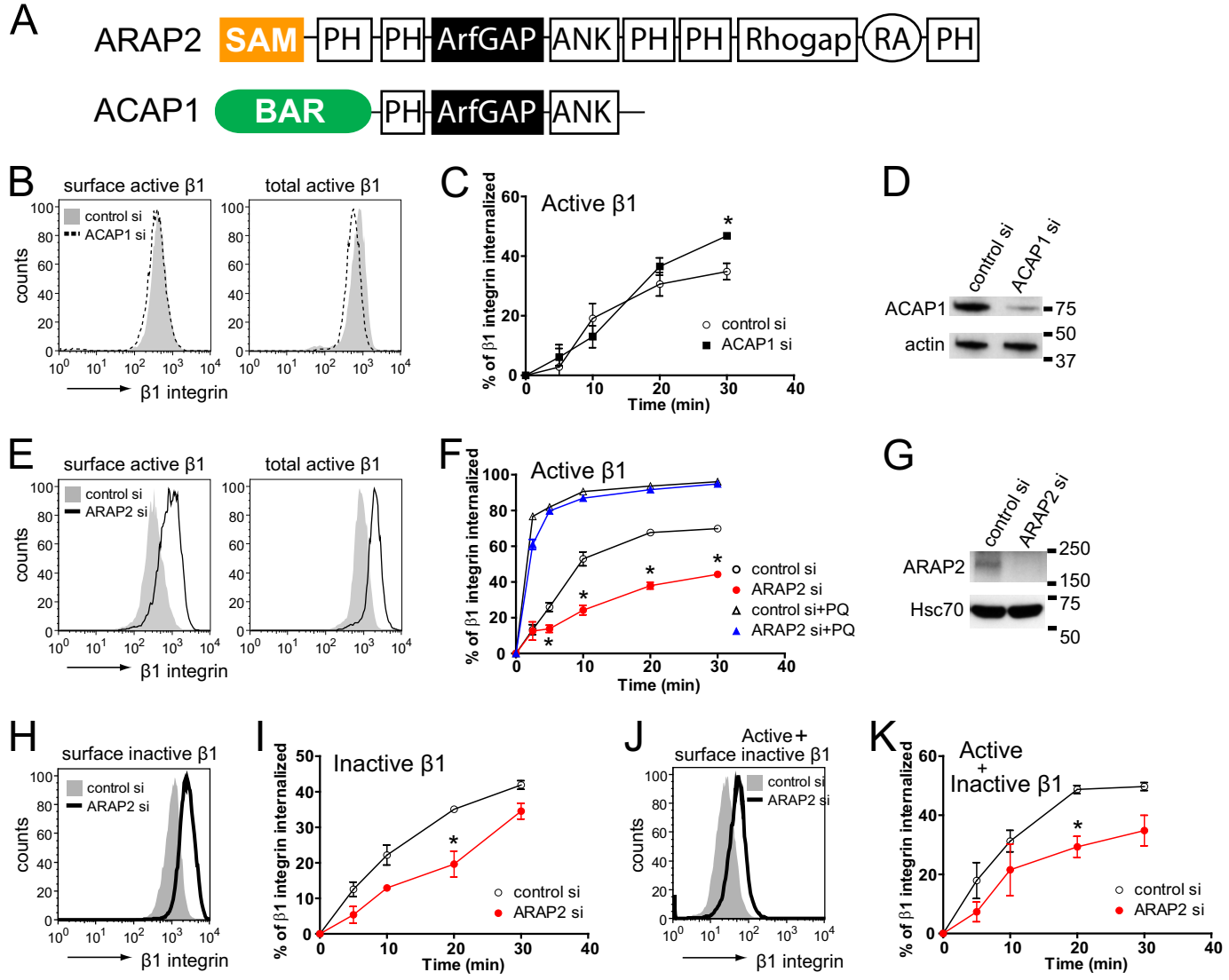

FIGURE 1. **ARAP2 and ACAP1 differentially affect endocytosis and recycling of β1 integrin.** *A*, schematic of the ARAP2 and ACAP1 domain structure. *SAM*, sterile α-motif; *ArfGAP*, ArfGTPase-activating protein; *Rhogap*, RhoGTPase-activating protein; *ANK*, ankyrin repeat; *RA*, Ras-association domain; *BAR*, *Bin/Amphiphysin/Rvs*. *B–K*, the net internalization rates of β1 integrin. siRNA-treated HeLa cells were labeled with an anti-active β1 integrin antibody (12G10), an anti-inactive β1 integrin antibody (MAB13), or an antibody that recognizes both the active and inactive forms of β1 integrin (MEM101A) at 4 °C, followed by incubation at 37 °C in the absence or presence of 0.3 mM primaquine (*PQ*). At each time point, surface β1 integrin was detected using a secondary antibody specific for the anti-β1 integrin antibody and flow cytometry. *B*, *E*, *H*, and *J*, representative FACS histograms from cells at time 0 (surface integrin) and from permeabilized cells (total integrin). *C*, *F*, *I*, and *K*, time dependence of integrin internalization. Results are mean ± S.E. from at least three experiments. *, $p < 0.05$. *D* and *G*, the efficiency of ARAP2 and ACAP1 knockdown was determined by immunoblot analyses.

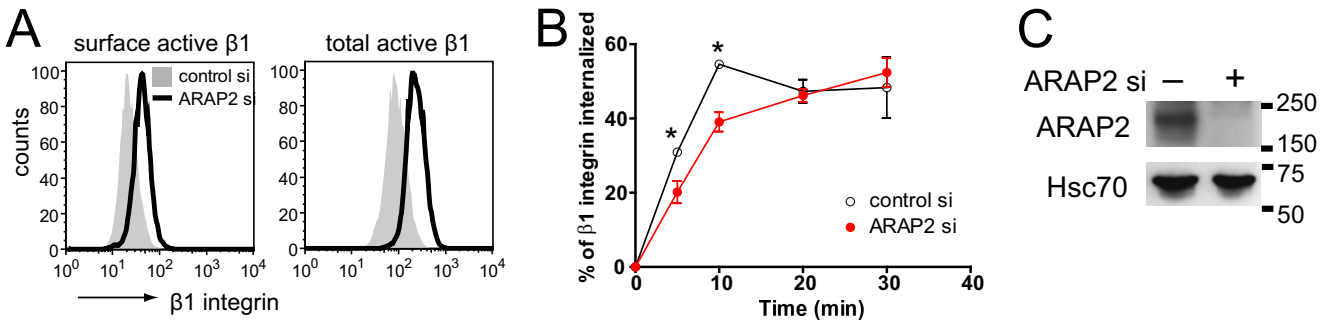

FIGURE 2. **ARAP2 affects the integrin traffic in MDA-MB-231 cells.** The internalization rates of active β1 integrin in siRNA-treated MDA-MB-231 cells were determined as in Fig. 1. Results shown are representative FACS histograms for surface and total active integrin (*A*) and time dependence of integrin internalization (*B*). *C*, efficiency of ARAP2 knockdown in MDA-MB-231 cells by immunoblotting. *, $p < 0.05$.

cells, the net rate and extent of integrin β1 internalization were 50~60% that of the control HeLa cells (Fig. 1*F*), and the difference from the control was observed within 5 min of initiating uptake. In MDA-MB-231 cells, ARAP2 knockdown also reduced the net internalization rate of integrin β1 (Fig. 2*B*). The effects of ARAP2 knockdown to increase integrin levels and to

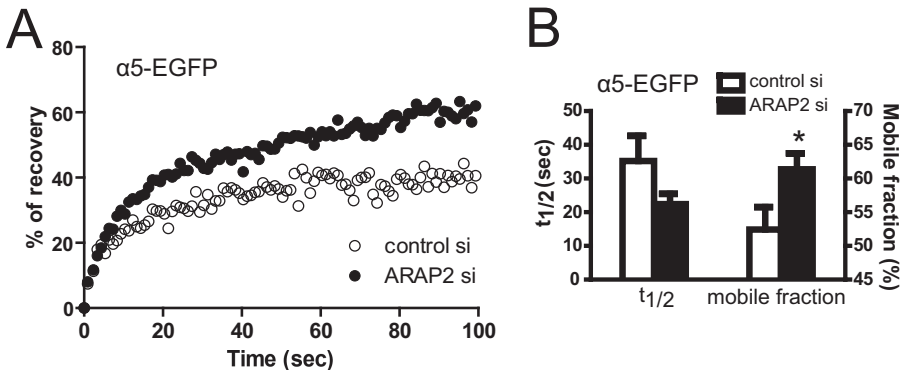

FIGURE 3. **ARAP2 modulates the exchange of integrin in FAs.** α5-EGFP and untagged β1 were expressed together in siRNA-treated HeLa cells. FRAP analysis was performed with a spinning disk microscope. *A*, example of α5-EGFP fluorescence recovery data. *B*, the average $t_{1/2}$ and mobile fraction of α5-EGFP fluorescence recovery in control siRNA ($n = 38$) and ARAP2 siRNA-transfected cells ($n = 39$, mean ± S.E.). *, $p < 0.05$.

slow the net rate of integrin internalization were independent of the activation state of integrin β1 because these results were also observed when using an antibody specific for inactive β1 or an antibody that does not discriminate between active and inactive β1 (Fig. 1, *H–K*).

The net rate of internalization is a balance of endocytosis and recycling. Therefore, a slower net rate of integrin internalization in ARAP2 knockdown cells could be due to reduced endocytosis or accelerated rapid recycling (29). In the presence of primaquine (*PQ*), which blocks recycling, therefore isolating endocytosis (30), the integrin endocytic rate in ARAP2 knockdown cells was indistinguishable from that in control cells (Fig. 1*F*). Therefore, the reduction in the net internalization rate in ARAP2 knockdown cells was likely due to accelerated recycling, in contrast to the effect of ACAP1 knockdown of slowing recycling (28). Because endocytosis occurred rapidly compared with the time resolution of the experiment, we cannot exclude an effect of ARAP2 on endocytosis on the basis of this experiment.

For further information on endocytosis, at least at FAs, we determined the exchange rate of integrin at FAs by FRAP analysis using α5-EGFP as a model integrin. α5-EGFP integrin was coexpressed with untagged β1 integrin in cells treated with control or ARAP2 siRNA. In Fig. 3*A*, example FRAP results for control and ARAP2 knockdown cells are shown. In Fig. 3*B*, the averages of $t_{1/2}$ for recovery and mobile fraction determined from 38 traces for control cells and 39 traces for ARAP2 knockdown cells are shown. The fluorescence recovery time of α5-EGFP was shorter and the exchangeable fraction of α5-EGFP was larger in ARAP2 knockdown cells (Fig. 3). This result is consistent with more rapid endocytosis and recycling rates of integrin in ARAP2 knockdown cells.

We examined additional cargos that transit the endocytic pathway. Following endocytosis, most transferrin receptor is recycled. We found that neither ARAP2 knockdown nor ACAP1 knockdown had a detectable effect on transferrin recycling (Fig. 4, *A* and *B*). The result with ACAP1 is different from that reported previously (22), which could be the result of a difference in the cell strain used or methodology. We also examined EGFR. Following receptor occupancy and endocytosis, EGFR is primarily targeted to the lysosome for degradation. We measured the rate of EGFR degradation to determine the effects on this pathway (31). Different from integrins, neither the total EGFR level nor the EGFR degradation rate was affected by ARAP2 knockdown or ACAP1 knockdown (Fig. 4, *C* and *D*).

ARAP2 Affects the Transit of Integrins from APPL to EEA1 Endosomes—We characterized the intracellular itinerary of integrins in HeLa cells with reduced ARAP2 expression. APPL1/2 is recruited by Rab5 and Rab21 to pre-early endosomes that form immediately after clathrin-dependent endocytosis. Subsequently, EEA1 is recruited to form the canonical early endosome that sorts transmembrane cargo proteins to various endosomal compartments, including the tubular recycling endosome that is positive for Rab11 and Rab22 (5, 32). ACAP1 has been reported to affect traffic of integrins through the tubular recycling compartment (11, 22, 28). To determine the step in the endocytic pathway affected by ARAP2, cells with reduced expression of ARAP2 were coimmunostained for β1 integrins and either endogenous APPL or endogenous EEA1 (Fig. 5). β1 integrins and APPL colocalized to a greater extent in HeLa cells with reduced ARAP2 than controls (Fig. 5, *A* and *C*). Similar results were obtained in the breast cancer cell line MDA-MB-231 (Fig. 5*D*). β1 integrin was also stained in control and ARAP2 knockdown cells expressing Rab5-GFP or Rab21-mCherry (Fig. 5*E*). Similar trends of more association of β1 integrin with these Rab5 family proteins were observed when ARAP2 was knocked down, although the data were not as clear, possibly because of the heterogeneity of the Rab5 compartment, which includes both APPL and EEA1 compartments. In contrast, the association of β1 integrins with EEA1 decreased in ARAP2 knockdown cells (Fig. 5, *B* and *C*). This reciprocal change in integrin association with APPL and EEA1 endosomes was observed for both active and inactive integrins (Fig. 5, *C* and *E*). β1 integrins no longer accumulated in APPL endosomes when FLAG-tagged wild-type ARAP2 was overexpressed in ARAP2 knockdown cells. ArfGAP-dead FLAG-[R728K]-ARAP2 did not rescue the defect (Fig. 5, *A* and *C*). From EEA1 endosomes, integrins can be sorted to the late endosomes/lysosomes or recycling compartments containing Rab4 or Rab11 (5, 33). In ARAP2 knockdown cells, colocalization of active β1 integrins with lysosomes (LAMP1) decreased (Fig. 5*E*), which may explain increased cellular levels of integrin (Fig. 1). We did

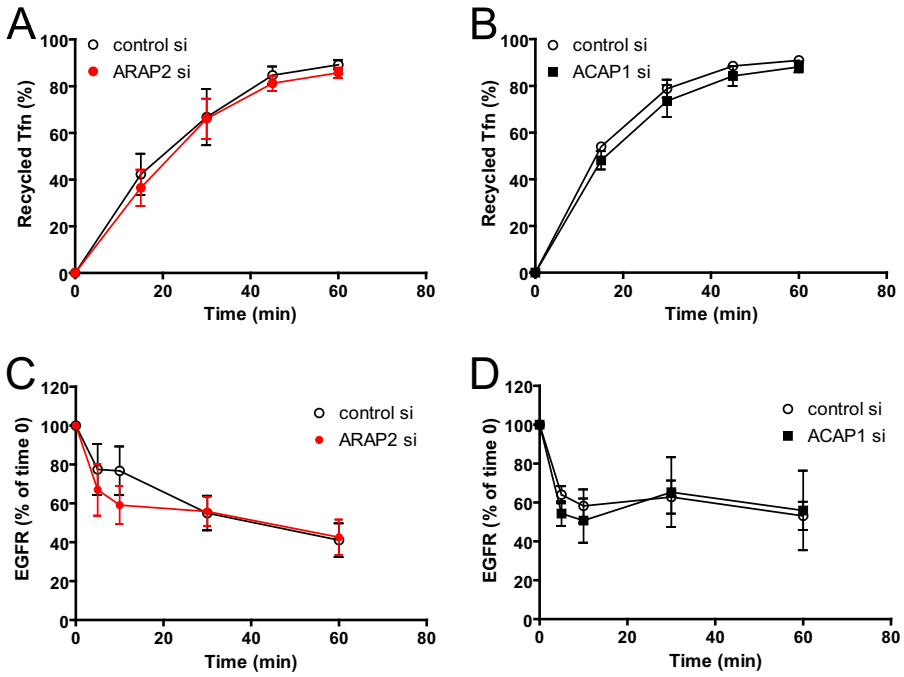

FIGURE 4. **Effects of ARAP2 or ACAP1 knockdown on traffic of transferrin and EGFR.** *A* and *B*, transferrin (*Tfn*) recycling. Transferrin-Alexa Fluor 488 was internalized in siRNA-treated HeLa cells at 37 °C for 30 min. Cells were washed and incubated in fresh media for the indicated times. Cells were put on ice, and internal transferrin-Alexa Fluor 488 was measured by flow cytometry. *C* and *D*, EGFR degradation. siRNA-treated HeLa cells were serum-starved overnight and subsequently treated with EGF for the indicated times. Cells were lysed, and EGFR levels were determined by anti-EGFR immunoblot analyses. Quantifications by densitometry analysis from three experiments (mean ± S.E.) are shown.

not detect differences in integrin association with Rab4 or Rab11 in ARAP2 knockdown cells (Fig. 5*E*).

ARAP2 also affected the cellular distribution of the APPL compartment. In both HeLa and MDA-MB-231 cells, APPL1-positive structures are distributed throughout the cells (Fig. 5). A small fraction of the cells had the APPL1 signal restricted to the periphery. Reducing ARAP2 expression in HeLa (Fig. 5, *F* and *G*) and MDA-MB-231 cells (Fig. 5*H*) increased the percentage of cells with peripheral APPL endosomes, further supporting the idea that ARAP2 regulates the APPL compartment.

ARAP2 Associates with an APPL1/Arf6-positive Compartment Morphologically Distinct from the ACAP1 Compartment—We compared the cellular distributions of ARAP2 and ACAP1 relative to APPL and Arf6 in the absence and presence of AlF_4^-, which can form a stable membrane-associated Arf6·GDP·AlF_4^-·ArfGAP complex (34). In the absence of AlF_4^-, GFP-APPL and FLAG-ARAP2 colocalized in punctate structures with Arf6-HA (Fig. 6*A*, Pearson's coefficient 0.20 ± 0.061). In cells expressing Arf6-HA with FLAG-ARAP2 and GFP-APPL1 and treated with AlF_4^-, the three proteins colocalized in membrane protrusions (Fig. 6, *A* and *B*, Pearson's coefficient 0.24 ± 0.051 for FLAG-ARAP2 and GFP-APPL1). In cells expressing FLAG-ACAP1, GFP-APPL1, and Arf6-HA and treated with AlF_4^-, ACAP1 colocalized with Arf6 in tubules that had terminal expansions enriched in GFP-APPL1 (Fig. 6*B*). The tubules were not observed in cells expressing ARAP2 instead of ACAP1. In cells coexpressing FLAG-ARAP2 and GFP-ACAP1, ARAP2 and ACAP1 did not colocalize in the tubular structures (Fig. 6*C*).

Examination of complex formation with APPL also revealed differences between ARAP2 and ACAP1. FLAG-ARAP2 and FLAG-ACAP1 were immunoprecipitated from lysates of cells expressing GFP-APPL1 and either FLAG-ARAP2 or FLAG-ACAP1 with an anti-FLAG antibody. GFP-APPL1 was detected in the precipitates from cells coexpressing FLAG-ARAP2 but not in precipitates from cells expressing GFP-APPL1 alone or GFP-APPL1 with ACAP1 (Fig. 6*D*). Similarly, when GFP-APPL1 was immunoprecipitated, more than 3% input of FLAG-ARAP2 was detected in the precipitates (Fig. 6*E*, note that the input signal is light, indicated by the *asterisk* in the *second lane from the right*). FLAG-ACAP1 was also present in these precipitates, but the precipitation was less efficient, with less than 3% of the input FLAG-ACAP1 present. Finally, endogenous APPL1 was also coimmunoprecipitated with endogenous ARAP2 (Fig. 6*F*), supporting the conclusion that ARAP2 associates with APPL1 in cells.

Cell morphology was differentially affected by ARAP2 and ACAP1. In the experiments determining whether ARAP2 and ACAP1 associated with different cellular structures, the cell morphology appeared to be related to the GAP that was expressed (Fig. 6). Furthermore, ACAP1 expression has been reported previously to prevent the formation of Arf6-induced protrusions (17). To determine whether ARAP2 also affects Arf6-dependent cell morphology, we compared cells expressing Arf6-HA alone or with either FLAG-ARAP2 or FLAG-ACAP1 and treated with AlF_4^- (Fig. 7). We classified Arf6-positive structures on the basis of morphology: ruffles, tubules, protrusions, and blebs (Fig. 7*A*). In the presence of AlF_4^-, Arf6-HA-expressing cells exhibited prominent membrane ruffles at the periphery and on the dorsal surface of the cell (Fig. 7, *A* and *B*, *Ruffles*), which were rarely seen when ARAP2 or ACAP1 was coexpressed with Arf6-HA. Expression of ARAP2 and ACAP1

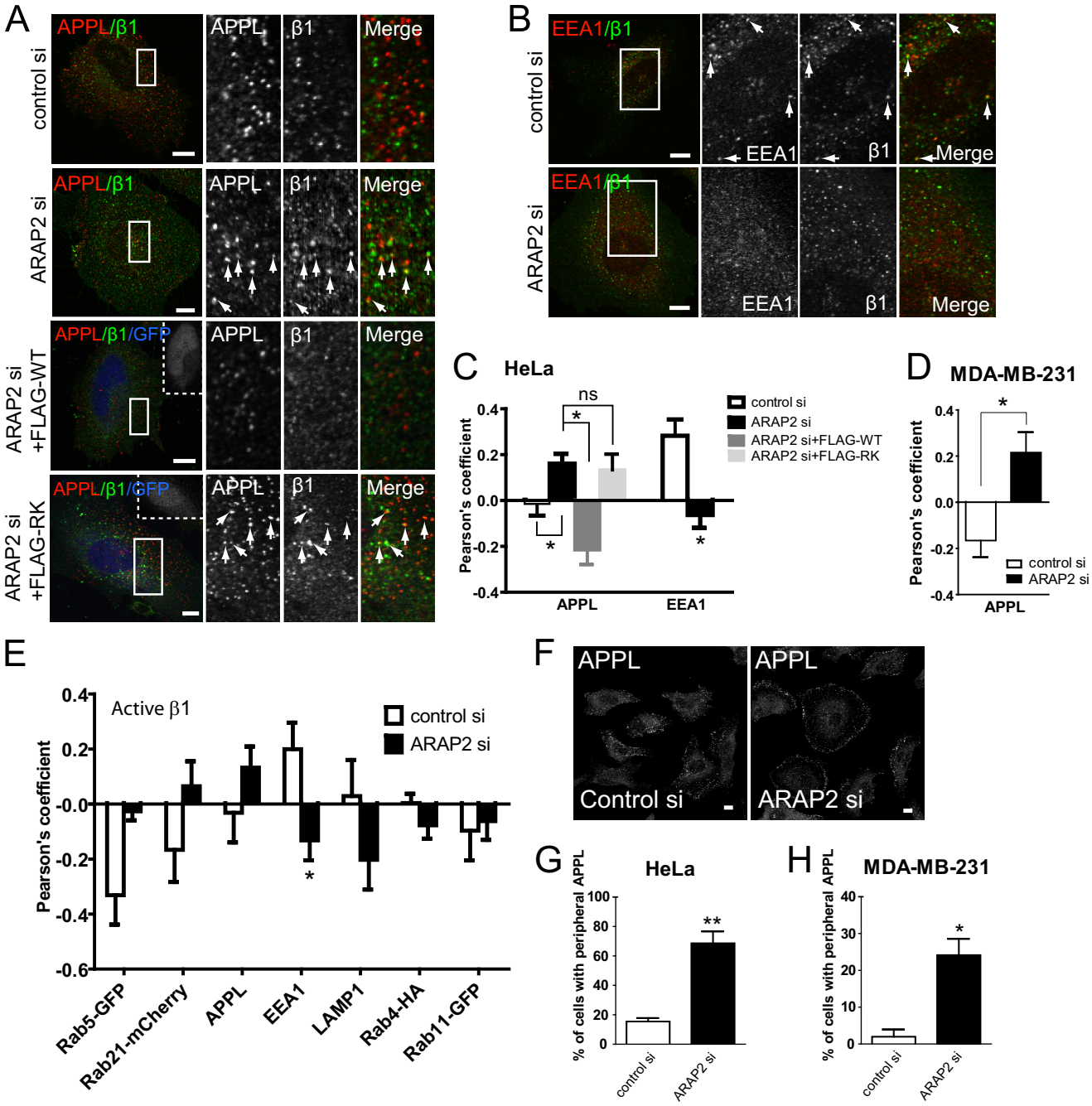

FIGURE 5. **ARAP2 controls integrin traffic from APPL to EEA1 endosomes.** *A–D*, colocalization of integrin with APPL or with EEA1 was examined. siRNA-treated HeLa and MDA-MB-231 cells expressing ARAP2 (*FLAG-WT*, *FLAG-RK*) and EGFP bicistronically or EGFP alone were costained for inactive β1 integrin (MAB13) and APPL or EEA1. Transfected cells were identified by GFP in the nucleus (shown in *blue* and in *white boxes*). *Boxed areas* are shown in higher magnification, with *arrows* indicating structures where colocalization was detected. Representative images (*A* and *B*) and quantification of colocalization between integrin and APPL or EEA1 (*C* and *D*) are shown ($n = 20\sim41$) from at least three experiments. *Scale bars* = 10 μm. *ns*, not significant. *, $p < 0.05$. *E*, ARAP2 affects the association of active integrin with organelles in the endocytic pathway. siRNA-treated HeLa cells were coimmunostained for active β1 integrin (9EG7) and markers for different organelles: APPL, EEA1, and LAMP1. Alternatively, siRNA-treated cells were transfected with plasmids for expressing different Rab proteins and stained for active β1 integrin (9EG7 or 12G10). *, $p < 0.05$. *F–H*, ARAP2 affects the cellular distribution of APPL endosomes. siRNA-treated HeLa and MDA-MB-231 cells were stained for APPL. The distribution of APPL was scored blindly as peripheral or non-peripheral for 40~80 cells from each group in each experiment. Representative images from HeLa cells (*F*) and quantification presented as the mean ± S.E. from three experiments (*G* and *H*) are shown. *Scale bars* = 10 μm. *, $p < 0.05$; **, $p < 0.005$.

induced different Arf6-positive structures. ARAP2 promoted membrane protrusions/blebs, whereas ACAP1 increased tubules (Fig. 7, *A* and *B*).

The tubules and protrusions induced by ACAP1 and ARAP2 were dependent on Arf6·GTP. Neither formed in AlF_4^--treated cells expressing ACAP1 or ARAP2 with a dominant negative mutant of Arf6 ([N122I]Arf6-HA) (Fig. 7, *C–E*). We conclude that the formation of protrusions and blebs depend on ARAP2 together with active Arf6, whereas tubules depend on active Arf6 with ACAP1.

Distinct Effects of ARAP2 and ACAP1 on FAs—We compared the effect of ARAP2 and ACAP1 overexpression on the size of

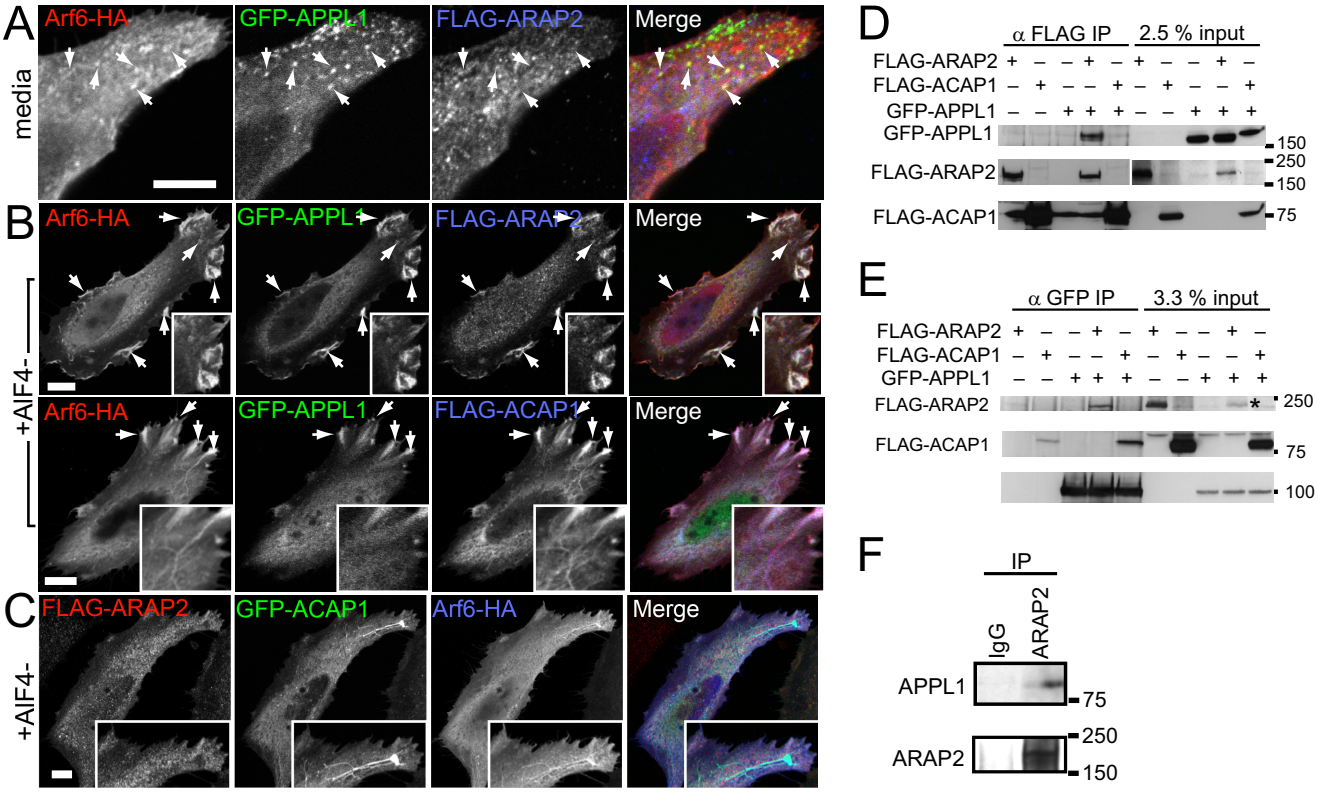

FIGURE 6. **Differential association of ARAP2 and ACAP1 with APPL.** *A–C*, localization of ARAP2 and ACAP1 relative to APPL and to each other. *A* and *B*, HeLa cells expressing Arf6-HA, GFP-APPL1, and either FLAG-ARAP2 or FLAG-ACAP1 were treated with (*B*) or without (*A*) AlF_4^- for 30 min, fixed, and stained with anti-HA and anti-FLAG antibodies. *C*, HeLa cells expressing FLAG-ARAP2, GFP-ACAP1, and Arf6-HA and treated with AlF_4^- were examined. A higher magnification is shown in *insets*, and *arrows* indicate structures where colocalization was detected. *Scale bars* = 10 μm. *D* and *E*, differences in ARAP2-APPL1 and ACAP1-APPL1 complex formation. Lysates from HeLa cells expressing FLAG-ARAP2 or FLAG-ACAP1 alone and in combination with GFP-APPL1 were immunoprecipitated (*IP*) through the FLAG epitope or GFP followed by immunoblotting using anti-GFP and anti-FLAG antibodies. The *asterisk* indicates the band representing FLAG-ARAP2 input in double-transfected cells. *F*, association of endogenous ARAP2 with APPL1. Endogenous ARAP2 was immunoprecipitated from HeLa lysates, followed by anti-APPL immunoblotting.

FAs using vinculin as a marker. ARAP2 overexpression resulted in fewer small adhesions and more large adhesions (>3 μm^2) (Fig. 8, *A* and *B*). In contrast, ACAP1 overexpression reduced all adhesions (Fig. 8, *A* and *B*). The expression levels of the recombinant ARAP2 were estimated to be 200- to 500-fold higher than that of endogenous ARAP2 (Fig. 8*C*). However, ARAPs are highly regulated (35), which would limit extreme effects of overexpression. In fact, ARAP2 knockdown has been reported previously to reduce FA size and number (36), consistent with our result in which overexpression resulted in larger FAs. Neither ARAP2 nor ACAP1 overexpression had a significant effect on total or surface active integrins (Fig. 8*D*). However, the overexpressed ARAP2 and ACAP1 associated with specific Arf6 compartments and had distinct effects on FAs. Therefore, the effect on the morphology of Arf6 structures and FAs cannot be explained by different amount of integrins and is not likely due to a nonspecific effect of the Arf GAP on Arf6 function. Rather, our results are consistent with the idea that a reduction in recycling by ARAP2 overexpression and accelerated recycling by ACAP1 overexpression may explain the effects on FAs because rapid recycling of $\alpha5\beta1$ has been reported to destabilize adhesions (12). We conclude that ARAP2 and ACAP1 are Arf6 GAPs that associate with different Arf6-positive endosomal compartments and have different effects on integrin traffic and opposing effects on FA morphology.

DISCUSSION

We examined two Arf6 GAPs to understand the opposing effects of Arf6 on integrins and integrin-dependent cellular processes. Arf6 and Arf6 exchange factors have been reported to affect both integrin endocytosis and exocytosis (11–13, 26), leading to the idea that Arf6 may affect integrin traffic at two distinct sites. We found that ARAP2 and ACAP1, two *bona fide* Arf6 GAPs, localize to morphologically distinct compartments and differentially affect integrin traffic and FAs. The Arf GAPs may, at least in part, define the Arf6 compartment and action.

The precise relationship of the ARAP2/APPL/Arf6 compartment within the complex traffic pathways of integrins remains to be fully characterized. Integrins are endocytosed into vesicles that fuse with a pre-early endosome. Some pre-early endosomes contain APPL. From the pre-early endosome, integrins are transported to the early endosome. Consistent with the accumulation of integrin in the APPL compartment in ARAP2 knockdown cells, ARAP2 may promote pre-early to early endosome traffic (Fig. 9, *route A*). From the early endosome, integrin is transported to either the degradative pathway or the recycling pathway and may be recycled from either (1, 33). A block in pre-early endosome to early endosome transport in ARAP2 knockdown cells would explain the result of decreased transit through the degradative pathway and increased total integrin

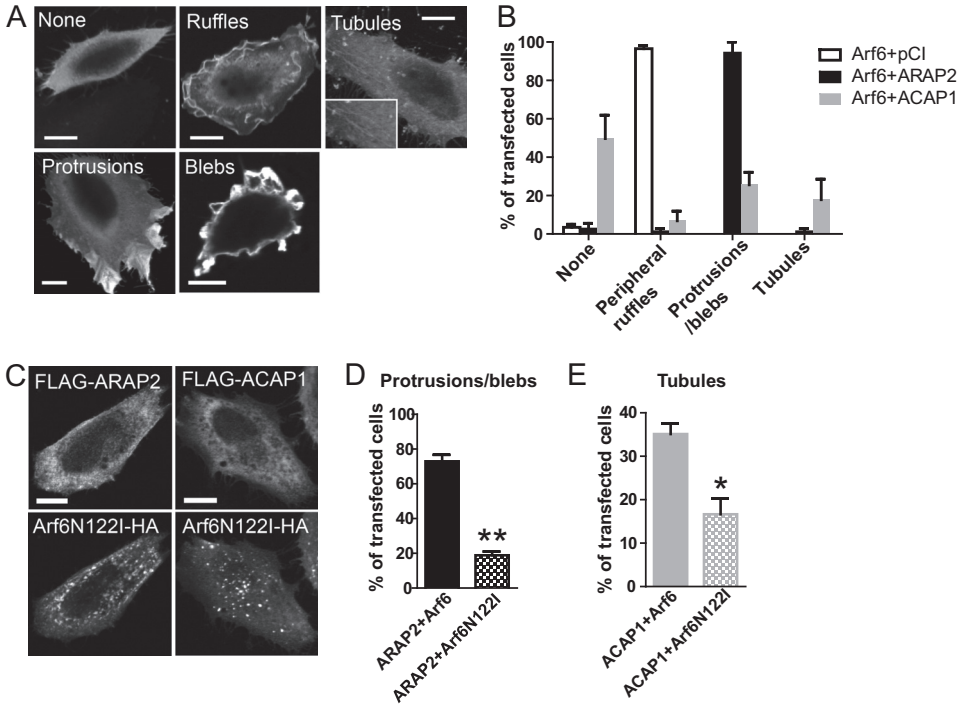

FIGURE 7. **Effects of ARAP2 and ACAP1 on Arf6-positive structures in cells treated with AlF_4^-.** HeLa cells transfected with Arf6-HA alone (*Arf6+pCI vector*) or together with FLAG-ARAP2 or FLAG-ACAP1 were treated with AlF_4^- for 30 min, fixed, and stained with anti-HA and anti-FLAG antibodies. *A*, representative images of various Arf6-positive structures by anti-HA staining. *B*, anti-HA staining images were scored blindly as different Arf6 structures for 20∼55 cells from each group in each experiment. The results shown are quantifications (mean ± S.E.) from two experiments. *C–E*, ARAP2- and ACAP1-induced structures depend on active Arf6. HeLa cells expressing [N122I]Arf6-HA with FLAG-ARAP2 or FLAG-ACAP1 were treated as in *A*. Anti-FLAG staining images were scored blindly for 40∼70 cells in each experiments. Representative images (*C*) and quantification (mean ± S.E.) from two to three experiments (*D* and *E*) are shown. *Scale bars* = 10 μm. *, $p < 0.05$; **, $p < 0.01$.

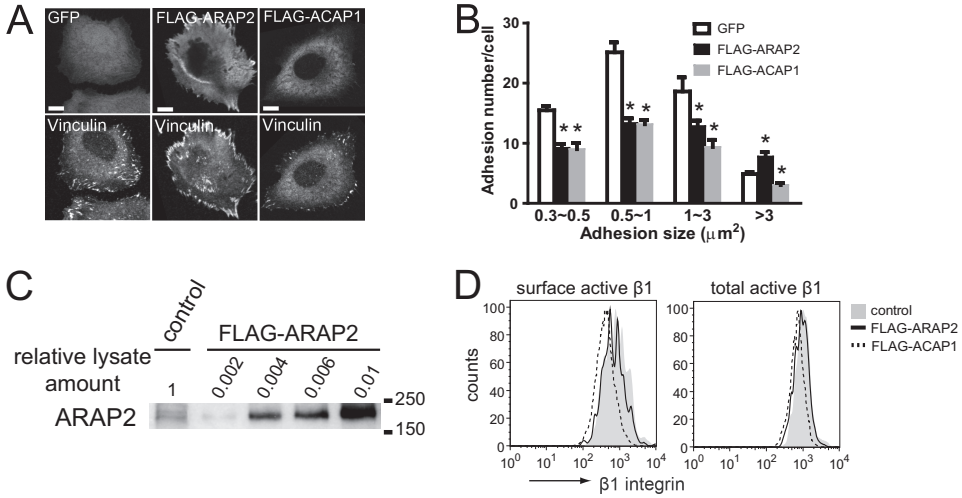

FIGURE 8. **ARAP2 and ACAP1 have different effects on FAs.** HeLa cells expressing GFP, FLAG-ARAP2, or FLAG-ACAP1 were plated on fibronectin-coated coverslips for 6 h, fixed, and stained with anti-vinculin and anti-FLAG antibodies. *A*, representative images. *B*, adhesion number and size expressed as the mean ± S.E. of at least three experiments. *Scale bars* = 10 μm. *, $p < 0.05$. *C*, levels of recombinant ARAP2 expression relative to endogenous ARAP2. Various amounts of lysates from HeLa cells transfected with FLAG-ARAP2 were analyzed concurrently with 45 μg of lysates from vector-transfected cells by anti-ARAP2 immunoblots to determine fold overexpression of FLAG-ARAP2. *D*, representative FACS histogram for surface and total active integrin in HeLa cells transfected with vector control, FLAG-tagged ARAP2, or ACAP1.

levels. The accelerated recycling rate may be the result of transport directly from the pre-early endosome to the tubular recycling compartment (6, 8) or transport from the APPL endosome to the plasma membrane (Fig. 9, *routes B* and *C*). It is plausible that ARAP2 prevents transport from pre-early endosome to tubular recycling endosome or to the plasma membranes and that knockdown of ARAP2 would, therefore, accelerate transport through these two routes (Fig. 9, *routes B* and *C*). Alternatively, with a block in transport of integrin from the pre-early endosome to the early endosome, the tubular recycling compartment or direct transport to the plasma membrane may be a default pathway for transport. Regardless of the specific path, as far as we are aware, this is the first report of an Arf GAP regulating the APPL compartment.

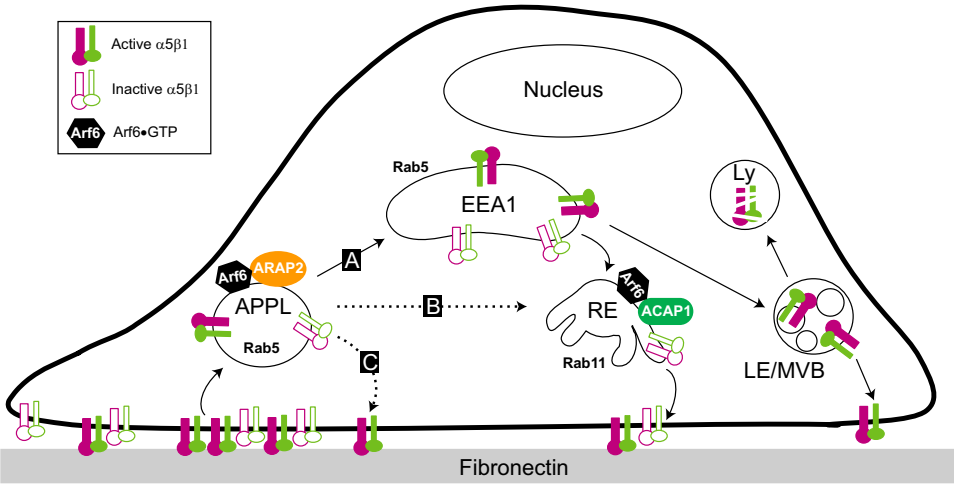

FIGURE 9. **Model for the sites of action of ARAP2 and ACAP1 in the endocytic pathway.** One Arf6 GAP, ARAP2, associates with APPL1 and controls the traffic of integrins from APPL endosomes. ARAP2 may promote integrin traffic from APPL to EEA1 early endosomes (*route A*) or prevent integrin transport from APPL directly to tubular recycling endosomes (*route B*) or to the plasma membrane (*route C*), leading to reduced α5β1 recycling. In contrast, another Arf6 GAP, ACAP1, localizes to tubular recycling endosomes and promotes α5β1 recycling. *RE*, recycling endosome; *Ly*, lysosome; *LE/MVB*, late endosome/multivesicular body.

Arf6 function in a pre-early endosome has been described previously in reports examining the effects of expressing constitutively active Arf6 (37). Arf6 associated with two compartments. One was the recycling endosome that also contained ACAP and Rab11 (4, 38). The other compartment was enriched in phosphatidylinositol 4,5-bisphosphate and trapped cargos (37, 39). The structure was assumed to have formed early during endocytosis. A plausible connection is that this phosphatidylinositol 4,5-bisphosphate-rich Arf6 compartment matures into the APPL/ARAP2/Arf6 compartment.

The mechanism responsible for the morphological differences in the Arf6-positive compartments in cells expressing ARAP2 or ACAP1 and treated with AlF_4^- remains elusive. ARAP2 or ACAP1 could generate the structures via an unique domain. For example, the *Bin/Amphiphysin/Rvs* domain of ACAP1 could induce the curvature necessary for the tubules to form. Alternatively, the inability to hydrolyze GTP on Arf6 because the GAP is sequestered in the Arf6•GDP•$AlF4^-$•GAP complex stabilizes or expands the specific GAP compartment.

The association of ARAP2 with an APPL/Arf6-positive compartment that regulates integrin traffic links several previous studies. APPL, which associates with very early endosomes, has been implicated in FA dynamics through its interaction with GAIP-interacting protein C terminus, member 1 (GIPC1, which binds to integrins (9)) to control integrin traffic and as an element of signaling that regulates FA dynamics (40). Arf6 has been reported to control integrin recycling and adhesion (11, 13, 29) and has been found to function downstream of syndecan4 to direct the itinerary of specific integrins to control FA dynamics (12). Increased Arf6•GTP levels accelerated α5β1 integrin recycling, destabilizing FAs, whereas decreased Arf6•GTP levels increased αvβ3 recycling, stabilizing FAs. ARAP2 could respond to cellular signals to regulate Arf6 and APPL in an endosomal compartment that controls the integrin traffic itinerary, therefore providing a single model explaining these reports.

Cargo sorting may be a common feature of Arf-dependent trafficking steps. We found that ARAP2 specifically affects the trafficking of β1 integrin without effects on EGFR or transferrin. Similarly, ACAP1 is thought to regulate the traffic of specific cargos from the recycling endosome (10, 41). A role for ArfGAP1, functioning with a class 1 or 2 Arf, in the cargo sorting in Golgi-to-endoplasmic reticulum trafficking has also been described (42–44), and ArfGAP3, also with a class 1 or 2 Arf, is postulated to affect the traffic of specific cargo between the early and late endosomes (45). Arf1 and Arf5 have also been reported to affect FAs and integrin trafficking (23, 36). Particular Arf GAPs may provide the cargo specificity necessary to navigate the complex endocytic pathways. Particular Arf GAPs may also determine specific intracellular itineraries. ARAP2 and ACAP1 handle integrin α5β1 in common but affect different compartments with different consequences.

Thirty-one genes encode Arf GAPs in humans, many with multiple splice variants (15). In many cases, a clear Arf specificity for Arf GAPs has not been able to be determined. It is possible that the Arf GAPs may be promiscuous in this regard. The "wobble" in the Arf may provide additional Arf/Arf GAP pairs for fine regulation of membrane traffic, with both the specific Arf and the specific GAP determining the particular effect.

ARAP2 may also have a central role in signaling from the APPL/Arf6 compartment. Phosphoinositides may be affected through regulation of Arf6, which activates phosphatidylinositol phosphate kinase (46), and by ARAP binding to SHIP2, a phosphoinositol 5′phosphatase (47). ARAP2 also affects Rac1•GTP levels and is a target of Rho (18, 36). Given that ARAP2 integrates a number of signals, we envision ARAP2 to be a key regulatory component of a signaling and membrane traffic station defined by the presence of APPL and dependence on Arf6. A plausible model is that ARAP2 and ACAP1 respond differentially to cellular signals to control the integrin trafficking necessary for specific effects on cell migration.

In summary, we identify a unique Arf6/APPL/ARAP2 endosomal compartment that is distinct from the ACAP1 endosomal compartment. We propose that, in addition to sorting specific cargos, particular endocytic itineraries are mediated by

distinct compartments defined, at least in part, by particular Arf/Arf GAP pairs (Fig. 9).

Acknowledgments—We thank Drs. James Casanova, Martin Schwartz, and Victor W. Hsu for discussions; Dr. Hsu for the GFP-ACAP1 plasmid; Dr. Elizabeth Sztul for the Rab21-mCherry plasmid; and Dr. Julie Donaldson for a critical review of the manuscript.

REFERENCES

1. Jacquemet, G., Humphries, M. J., and Caswell, P. T. (2013) Role of adhesion receptor trafficking in 3D cell migration. *Curr. Opin. Cell Biol.* **25,** 627–632
2. D'Souza-Schorey, C., and Chavrier, P. (2006) ARF proteins: roles in membrane traffic and beyond. *Nat. Rev. Mol. Cell Biol.* **7,** 347–358
3. Donaldson, J. G. (2003) Multiple roles for Arf6: sorting, structuring, and signaling at the plasma membrane. *J. Biol. Chem.* **278,** 41573–41576
4. Maldonado-Báez, L., and Donaldson, J. G. (2013) Hook1, microtubules, and Rab22: mediators of selective sorting of clathrin-independent endocytic cargo proteins on endosomes. *Bioarchitecture* **3,** 141–146
5. Grant, B. D., and Donaldson, J. G. (2009) Pathways and mechanisms of endocytic recycling. *Nat. Rev. Mol. Cell Biol.* **10,** 597–608
6. Maldonado-Báez, L., Williamson, C., and Donaldson, J. G. (2013) Clathrin-independent endocytosis: a cargo-centric view. *Exp. Cell Res.* **319,** 2759–2769
7. Dozynkiewicz, M. A., Jamieson, N. B., Macpherson, I., Grindlay, J., van den Berghe, P. V., von Thun, A., Morton, J. P., Gourley, C., Timpson, P., Nixon, C., McKay, C. J., Carter, R., Strachan, D., Anderson, K., Sansom, O. J., Caswell, P. T., and Norman, J. C. (2012) Rab25 and CLIC3 collaborate to promote integrin recycling from late endosomes/lysosomes and drive cancer progression. *Dev. Cell* **22,** 131–145
8. Maldonado-Báez, L., Cole, N. B., Krämer, H., and Donaldson, J. G. (2013) Microtubule-dependent endosomal sorting of clathrin-independent cargo by Hook1. *J. Cell Biol.* **201,** 233–247
9. Valdembri, D., Caswell, P. T., Anderson, K. I., Schwarz, J. P., König, I., Astanina, E., Caccavari, F., Norman, J. C., Humphries, M. J., Bussolino, F., and Serini, G. (2009) Neuropilin-1/GIPC1 signaling regulates α 5 β 1 integrin traffic and function in endothelial cells. *PLoS Biol.* **7,** e25
10. Schuldt, A. (2012) Getting active: protein sorting in endocytic recycling. *Nat. Rev. Mol. Cell Biol.* **13,** 1–6
11. Powelka, A. M., Sun, J., Li, J., Gao, M., Shaw, L. M., Sonnenberg, A., and Hsu, V. W. (2004) Stimulation-dependent recycling of integrin β 1 regulated by ARF6 and Rab11. *Traffic* **5,** 20–36
12. Morgan, M. R., Hamidi, H., Bass, M. D., Warwood, S., Ballestrem, C., and Humphries, M. J. (2013) Syndecan-4 phosphorylation is a control point for integrin recycling. *Dev. Cell* **24,** 472–485
13. Sakurai, A., Gavard, J., Annas-Linhares, Y., Basile, J. R., Amornphimoltham, P., Palmby, T. R., Yagi, H., Zhang, F., Randazzo, P. A., Li, X., Weigert, R., and Gutkind, J. S. (2010) Semaphorin 3E initiates antiangiogenic signaling through Plexin D1 by regulating Arf6 and R-Ras. *Mol. Cell. Biol.* **30,** 3086–3098
14. Parsons, J. T., Horwitz, A. R., and Schwartz, M. A. (2010) Cell adhesion: integrating cytoskeletal dynamics and cellular tension. *Nat. Rev. Mol. Cell Biol.* **11,** 633–643
15. Kahn, R. A., Bruford, E., Inoue, H., Logsdon, J. M., Jr., Nie, Z., Premont, R. T., Randazzo, P. A., Satake, M., Theibert, A. B., Zapp, M. L., and Cassel, D. (2008) Consensus nomenclature for the human ArfGAP domain-containing proteins. *J. Cell Biol.* **182,** 1039–1044
16. Kahn, R. A., Cherfils, J., Elias, M., Lovering, R. C., Munro, S., and Schurmann, A. (2006) Nomenclature for the human Arf family of GTP-binding proteins: ARF, ARL, and SAR proteins. *J. Cell Biol.* **172,** 645–650
17. Jackson, T. R., Brown, F. D., Nie, Z., Miura, K., Foroni, L., Sun, J., Hsu, V. W., Donaldson, J. G., and Randazzo, P. A. (2000) ACAPs are Arf6 GTPase-activating proteins that function in the cell periphery. *J. Cell Biol.* **151,** 627–638
18. Yoon, H. Y., Miura, K., Cuthbert, E. J., Davis, K. K., Ahvazi, B., Casanova, J. E., and Randazzo, P. A. (2006) ARAP2 effects on the actin cytoskeleton are dependent on Arf6-specific GTPase-activating-protein activity and binding to RhoA-GTP. *J. Cell Sci.* **119,** 4650–4666
19. Ha, V. L., Luo, R., Nie, Z., and Randazzo, P. A. (2008) Contribution of AZAP-type Arf GAPs to cancer cell migration and invasion. *Adv. Cancer Res.* **101,** 1–28
20. Inoue, H., and Randazzo, P. A. (2007) Arf GAPs and their interacting proteins. *Traffic* **8,** 1465–1475
21. Randazzo, P. A., Inoue, H., and Bharti, S. (2007) Arf GAPs as regulators of the actin cytoskeleton. *Biol. Cell* **99,** 583–600
22. Dai, J., Li, J., Bos, E., Porcionatto, M., Premont, R. T., Bourgoin, S., Peters, P. J., and Hsu, V. W. (2004) ACAP1 promotes endocytic recycling: short article by recognizing recycling sorting signals. *Dev. Cell* **7,** 771–776
23. Moravec, R., Conger, K. K., D'Souza, R., Allison, A. B., and Casanova, J. E. (2012) BRAG2/GEP100/IQSec1 interacts with clathrin and regulates α 5 β 1 integrin endocytosis through activation of ADP ribosylation factor 5 (Arf5). *J. Biol. Chem.* **287,** 31138–31147
24. Chen, P. W., and Kroog, G. S. (2010) Leupaxin is similar to paxillin in focal adhesion targeting and tyrosine phosphorylation but has distinct roles in cell adhesion and spreading. *Cell Adh. Migr.* **4,** 527–540
25. Balasubramanian, N., Scott, D. W., Castle, J. D., Casanova, J. E., and Schwartz, M. A. (2007) Arf6 and microtubules in adhesion-dependent trafficking of lipid rafts. *Nat. Cell Biol.* **9,** 1381–1391
26. Dunphy, J. L., Moravec, R., Ly, K., Lasell, T. K., Melancon, P., and Casanova, J. E. (2006) The Arf6 GEF GEP100/13RAG2 regulates cell adhesion by controlling endocytosis of β 1 Integrins. *Curr. Biol.* **16,** 315–320
27. Sakurai, A., Jian, X., Lee, C. J., Manavski, Y., Chavakis, E., Donaldson, J., Randazzo, P. A., and Gutkind, J. S. (2011) Phosphatidylinositol-4-phosphate 5-kinase and GEP100/Brag2 protein mediate antiangiogenic signaling by Semaphorin 3E-Plexin-D1 through Arf6 protein. *J. Biol. Chem.* **286,** 34335–34345
28. Li, J., Ballif, B. A., Powelka, A. M., Dai, J., Gygi, S. P., and Hsu, V. W. (2005) Phosphorylation of ACAP1 by Akt regulates the stimulation-dependent recycling of integrin β 1 to control cell migration. *Dev. Cell* **9,** 663–673
29. Arjonen, A., Alanko, J., Veltel, S., and Ivaska, J. (2012) Distinct recycling of active and inactive ss 1 integrins. *Traffic* **13,** 610–625
30. Teckchandani, A., Toida, N., Goodchild, J., Henderson, C., Watts, J., Wollscheid, B., and Cooper, J. A. (2009) Quantitative proteomics identifies a Dab2/integrin module regulating cell migration. *J. Cell Biol.* **186,** 99–111
31. Tomas, A., Futter, C. E., and Eden, E. R. (2014) EGF receptor trafficking: consequences for signaling and cancer. *Trends Cell Biol.* **24,** 26–34
32. Miaczynska, M., Christoforidis, S., Giner, A., Shevchenko, A., Uttenweiler-Joseph, S., Habermann, B., Wilm, M., Parton, R. G., and Zerial, M. (2004) APPL proteins link Rab5 to nuclear signal transduction via an endosomal compartment. *Cell* **116,** 445–456
33. Caswell, P. T., and Norman, J. C. (2006) Integrin trafficking and the control of cell migration. *Traffic* **7,** 14–21
34. Luo, R., Ahvazi, B., Amariei, D., Shroder, D., Burrola, B., Losert, W., and Randazzo, P. A. (2007) Kinetic analysis of GTP hydrolysis catalysed by the Arf1-GTP-ASAP1 complex. *Biochem. J.* **402,** 439–447
35. Campa, F., Yoon, H. Y., Ha, V. L., Szentpetery, Z., Balla, T., and Randazzo, P. A. (2009) A PH Domain in the Arf GTPase-activating protein (GAP) ARAP1 binds phosphatidylinositol 3,4,5-trisphosphate and regulates Arf GAP activity independently of recruitment to the plasma membranes. *J. Biol. Chem.* **284,** 28069–28083
36. Chen, P. W., Jian, X., Yoon, H. Y., and Randazzo, P. A. (2013) ARAP2 signals through Arf6 and Rac1 to control focal adhesion morphology. *J. Biol. Chem.* **288,** 5849–5860
37. Brown, F. D., Rozelle, A. L., Yin, H. L., Balla, T., and Donaldson, J. G. (2001) Phosphatidylinositol 4,5-bisphosphate and Arf6-regulated membrane traffic. *J. Cell Biol.* **154,** 1007–1017
38. Chaineau, M., Ioannou, M. S., and McPherson, P. S. (2013) Rab35: GEFs, GAPs and Effectors. *Traffic* **14,** 1109–1117
39. Naslavsky, N., Weigert, R., and Donaldson, J. G. (2003) Convergence of non-clathrin-and clathrin-derived endosomes involves Arf6 inactivation and changes in phosphoinositides. *Mol. Biol. Cell* **14,** 417–431
40. Broussard, J. A., Lin, W. H., Majumdar, D., Anderson, B., Eason, B., Brown, C. M., and Webb, D. J. (2012) The endosomal adaptor protein APPL1

impairs the turnover of leading edge adhesions to regulate cell migration. *Mol. Biol. Cell* **23,** 1486–1499
41. Bai, M., Pang, X., Lou, J., Zhou, Q., Zhang, K., Ma, J., Li, J., Sun, F., and Hsu, V. W. (2012) Mechanistic insights into regulated cargo binding by ACAP1 protein. *J. Biol. Chem.* **287,** 28675–28685
42. Lanoix, J., Ouwendijk, J., Lin, C. C., Stark, A., Love, H. D., Ostermann, J., and Nilsson, T. (1999) GTP hydrolysis by arf-1 mediates sorting and concentration of Golgi resident enzymes into functional COPI vesicles. *EMBO J.* **18,** 4935–4948
43. Lanoix, J., Ouwendijk, J., Stark, A., Szafer, E., Cassel, D., Dejgaard, K., Weiss, M., and Nilsson, T. (2001) Sorting of Golgi resident proteins into different subpopulations of COPI vesicles: a role for ArfGAP1. *J. Cell Biol.* **155,** 1199–1212
44. Goldberg, J. (2000) Decoding of sorting signals by coatomer through a GTPase switch in the COPI coat complex. *Cell* **100,** 671–679
45. Shiba, Y., Kametaka, S., Waguri, S., Presley, J. F., and Randazzo, P. A. (2013) ArfGAP3 regulates the transport of cation-independent mannose 6-phosphate receptor in the post-Golgi compartment. *Curr. Biol.* **23,** 1945–1951
46. Honda, A., Nogami, M., Yokozeki, T., Yamazaki, M., Nakamura, H., Watanabe, H., Kawamoto, K., Nakayama, K., Morris, A. J., Frohman, M. A., and Kanaho, Y. (1999) Phosphatidylinositol 4-phosphate 5-kinase α is a downstream effector of the small G protein ARF6 in membrane ruffle formation. *Cell* **99,** 521–532
47. Raaijmakers, J. H., Deneubourg, L., Rehmann, H., de Koning, J., Zhang, Z., Krugmann, S., Erneux, C., and Bos, J. L. (2007) The PI3K effector Arap3 interacts with the PI(3,4,5)P-3 phosphatase SHIP2 in a sterile α-motif domain-dependent manner. *Cell Signal* **19,** 1249–1257